

# Seasonal climate summary southern hemisphere (autumn 2003): demise of the 2002/03 El Niño event

Grant S. Beard

National Climate Centre, Bureau of Meteorology, Australian  
(Manuscript received December 2003)

**Southern hemisphere circulation patterns and associated anomalies for the austral autumn 2003 are reviewed, with emphasis given to the Pacific Basin climate indicators and Australian rainfall and temperature patterns.**

**Autumn 2003 saw the complete demise of the El Niño event which began about one year earlier. Sustained cooling of surface waters occurred in the central to eastern tropical Pacific, and negative anomalies were widespread in the tropical Pacific sub-surface. Averaged over the season, the Walker circulation was enhanced and the amount of cloud around the equatorial dateline was generally close to average for the time of year.**

**Australian rainfall patterns returned to something closer to average, although seasonal falls in many instances were insufficient to provide a clear break to the severe drought conditions. Maximum temperatures were above average over large parts of the country, but there was close to an even split between positive and negative anomalies for seasonal minima.**

## Introduction

The El Niño event that began in autumn 2002 (Fawcett and Trewin 2003), concluded in autumn 2003 after signs of its demise first became apparent during the summer immediately prior (Reid 2003). Most of the key ENSO indicators such as trade winds, sea-surface temperatures, sub-surface ocean temperatures and high cloud amount, returned to neutral values as the season progressed. The Southern Oscillation Index was the only indicator to show little seasonal trend with weak negative values persisting during the March to May period.

In Australia, hopes were dashed for a widespread break to the severe drought as autumn rains were patchy following a wet February. Seasonal totals across much of the eastern half of the country were close to the long-term median in many instances, although some significant areas registered falls below the 30th percentile. Above average falls were mainly confined to eastern Tasmania, coastal NSW and the interior of WA.

Maximum temperatures tended to be above average, particularly in the northern half of the country as well as in southwest WA. In contrast, the Australia-wide seasonal minimum temperature anomaly was close to zero.

This summary reviews the southern hemisphere and equatorial climate patterns for autumn 2003, with particular attention given to the Australasian and

---

*Corresponding author address:* Grant. S. Beard, National Climate Centre, Bureau of Meteorology, GPO Box 1289K, Melbourne, Vic. 3001, Australia.  
Email: g.beard@bom.gov.au

Pacific regions. The main sources of information for this report are the *Climate Monitoring Bulletin* (Bureau of Meteorology, Australia) and the *Climate Diagnostics Bulletin* (Climate Prediction Center, Washington). Further details regarding sources of data are given in the Appendix.

## Pacific Basin climate indices

### The Troup Southern Oscillation Index\*

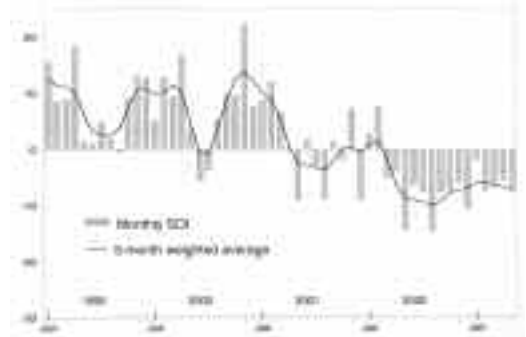
The sequence of negative Southern Oscillation Index (SOI) values in place at the end of summer (Reid 2003), continued during autumn 2003. The monthly values were  $-6.8$ ,  $-5.5$  and  $-7.4$  for March, April and May respectively, thereby giving a seasonal mean of  $-6.6$ .

These figures do however mask a considerable degree of intraseasonal variability. For example, an approximate 30-day running mean of the SOI dropped below  $-10$  in early April before rising steadily to small positive values by mid-May. This was then followed by a steady and consistent decline in the 30-day mean that was not arrested until the middle of June, by which time its value was approaching  $-20$ .

Darwin's mean sea-level pressure (MSLP) remained above the climatological normal for most of the season with positive anomalies being recorded for each autumn month. One notable exception to the general pattern occurred in mid-March when, for a brief period, the MSLP dropped to about 1001 hPa, some 6 hPa below average, in association with the development of tropical cyclone *Craig* off the north coast of the Northern Territory. Tahiti's MSLP fluctuated more vigorously than Darwin's and the individual monthly anomalies were  $-0.4$ ,  $+0.3$  and  $-0.5$  respectively. The five-month moving mean of the SOI became slightly more negative during the season, possibly suggesting a continuation of El Niño conditions, as least as far as atmospheric pressure was concerned. Figure 1 shows the monthly SOI values from January 1999 to May 2003. A curve of five-month moving averages has been superimposed on the graph.

The February/March, March/April and April/May values of the Climate Diagnostics Center (CDC) Multivariate El Niño-Southern Oscillation (ENSO) Index (MEI) (Wolter and Timlin 1993, 1998) were  $+0.817$ ,  $+0.377$  and  $+0.001$  respectively. These values were lower than the two positive values covering the summer period (Reid 2003), and indicate a relaxation

**Fig. 1** Southern Oscillation Index, from January 1999 to May 2003. Means and standard deviations used in the computation of the SOI are based on the period 1933-1992.



of El Niño conditions to a neutral state. The MEI is derived from a number of atmospheric and oceanic indicators, and typically shows positive values in excess of  $+0.8$  during El Niño events.

### Outgoing long wave radiation

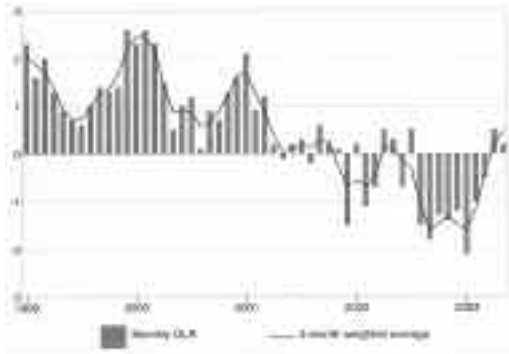
Figure 2, adapted from the Climate Prediction Center (CPC), Washington (CPC 2003), shows the standardised monthly anomaly of outgoing long-wave radiation (OLR) from January 1999 to May 2003, together with a three-month moving average. These data, compiled by the CPC, are a measure of the amount of long wave radiation emitted from an equatorial region centred about the date-line ( $5^{\circ}\text{S}$  to  $5^{\circ}\text{N}$  and  $160^{\circ}\text{E}$  to  $160^{\circ}\text{W}$ ). Tropical deep convection in this region is particularly sensitive to changes in the phase of the Southern Oscillation. During warm (El Niño) ENSO events, convection is generally more prevalent resulting in a reduction in OLR. This reduction is due to the lower effective black-body temperature and is associated with increased high cloud and deep convection. The reverse applies in cold (La Niña) events, with less convection expected in the vicinity of the date-line.

The monthly values  $-0.5$  (March),  $+0.5$  (April) and  $+0.2$  (May) of this index were consistent with a return to a neutral state of the Southern Oscillation. There was a period of substantially increased convection around the date-line in the second half of March, but following this, periods of negative OLR anomaly were few in number and low in magnitude in this region.

Activity associated with the Madden-Julian Oscillation (MJO) decreased in autumn following a

\*The Troup Southern Oscillation Index (SOI) used in this article is ten times the standardised monthly anomaly of the difference in mean sea-level pressure between Tahiti and Darwin. The calculation is based on a sixty-year climatology (1933-1992).

**Fig. 2** Standardised anomaly of monthly outgoing long wave radiation averaged over the area 5°S to 5°N and 160°E to 160°W, from January 1999 to May 2003. Negative (positive) anomalies indicate enhanced (reduced) convection and rainfall in the area. Anomalies are based on the 1979-1995 base period. After CPC (2003).



period of regular pulses during summer (Reid 2003). The MJO is characterised by waves of enhanced or suppressed convective activity propagating eastward across the Indian Ocean and northern Australian tropics to the western, or sometimes central, Pacific (Wheeler and Weickman 2001). The most notable passage of the MJO for the season occurred during early to mid-March when an eastward propagating area of enhanced convection spawned tropical cyclones *Craig* just north of Melville Island off the northern NT coast, and *Erica* in the Coral Sea.

Tropical cyclone *Erica* was arguably the most severe tropical cyclone to affect New Caledonia in 50 years, bringing gales and heavy rainfall to the country between 12 and 14 March, with a peak gust of 234 km/h. Parts of Noumea suffered the most, with damage estimates ranging up to 450 million Pacific francs. Also forming at around the same time was tropical cyclone *Eseta*, which passed Fiji on 13 March before weakening rapidly the following day and decaying by 15 March. Peak gusts were estimated to have reached 240 km/h. The only other tropical cyclone forming in the south Pacific during autumn was *Fili*, a very short-lived system that formed near 18°S 175°W on 15 April.

Tropical cyclone *Inigo* formed in the Timor Sea on 2 April and eventually crossed the northwest coast of Australia on the 8th. This particular storm does not appear to have been associated with an MJO event.

## Oceanic patterns

### Sea-surface temperatures

Figure 3 shows autumn 2003 sea-surface temperature (SST) anomalies in degrees Celsius (°C), derived from analyses obtained from the National Meteorological and Oceanographic Centre (NMOC). The contour interval is 0.5°C, but the zero contour is omitted. Positive anomalies are shown in orange and red shades, while negative anomalies are shown in blue shades.

The entire tropical Pacific cooled during autumn in line with the decaying El Niño event. In absolute terms, the decrease in the strength of the positive anomalies was less marked in the western Pacific than it was in the east of the basin. Anomalies remained positive for the duration of the season in the NINO4 region (western tropical Pacific), and a small region of +1 to +1.5°C departures was evident around the equatorial date-line for the seasonal mean.

Further east, the cooling trend was strong enough to cause the development of seasonally averaged negative anomalies in the equatorial Pacific cold tongue east of about 140°W. The NINO3 and NINO3.4 indices both dropped by 1.2°C between February and May, while the combined NINO1+2 index fell by 1.6°C over the same period. The NINO3.4 index represents the central tropical Pacific, NINO3 the central to eastern tropical Pacific, and NINOs 1 and 2 the far eastern tropical Pacific near the South American coast. With the NINO1+2 index standing at -1.8°C by season's end, there was some speculation in the international climate community about a possible La Niña event.

Around Australia the oceans were warmer than average, although the anomalies were generally small in magnitude. The Indian Ocean north of latitude 25°S was warmer than average in autumn, with +0.5 to +1.0°C anomalies stretching from south of India southeast to the Western Australian coast.

### Subsurface patterns

Figure 4 shows a time-longitude diagram of the anomaly in metres of the depth of the 20°C isotherm along the equatorial Pacific Ocean between January 1996 and May 2003, as calculated by the Bureau of Meteorology Research Centre (BMRC). The 20°C isotherm is generally situated close to the equatorial ocean thermocline, the region of greatest vertical temperature gradient with respect to depth. The thermocline can also be regarded as the boundary between the upper ocean warm water and the deeper ocean cold water. An abnormally shallow thermocline in the eastern Pacific Ocean is characteristic of La Niña events. Positive anomalies correspond to the 20°C isotherm being deeper than average, and negative anomalies to it being shallower than average.

Fig. 3 Anomalies of sea-surface temperature for autumn (March, April, May) 2003 ( $^{\circ}\text{C}$ ). The contour interval is  $0.5^{\circ}\text{C}$ .

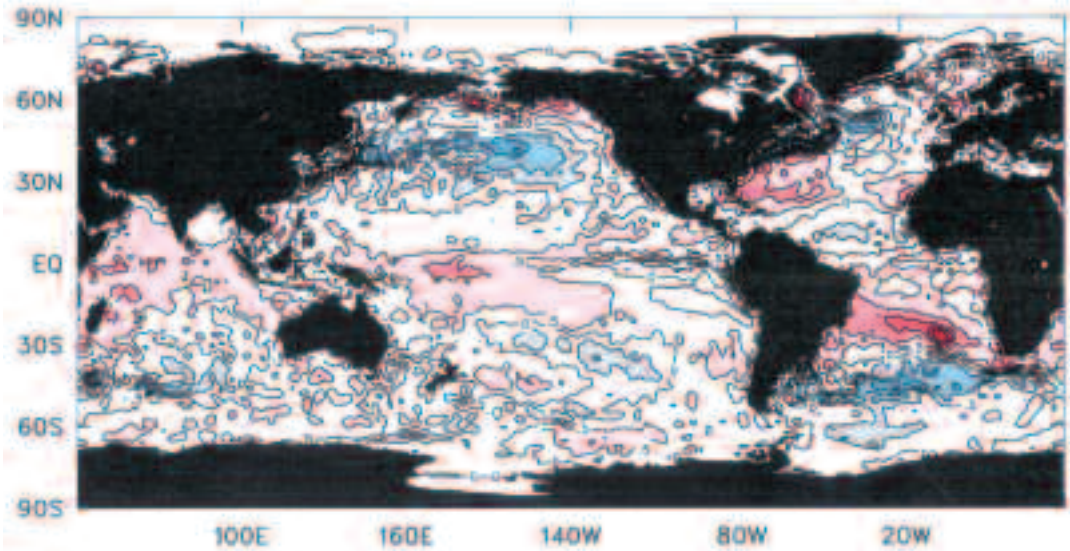
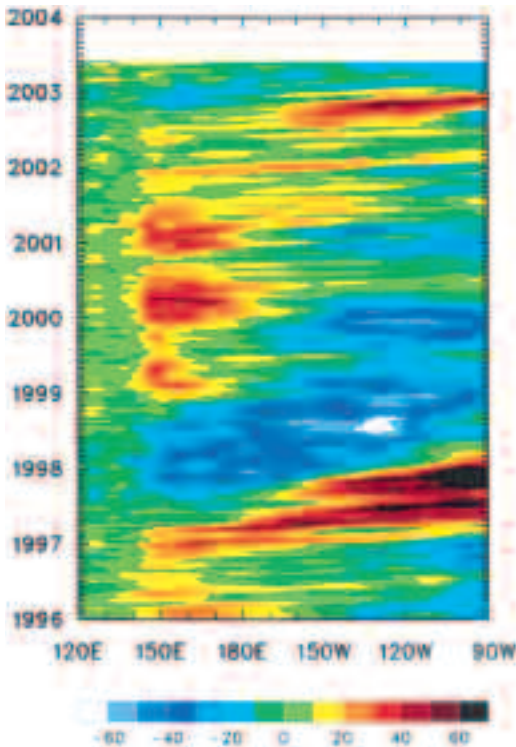


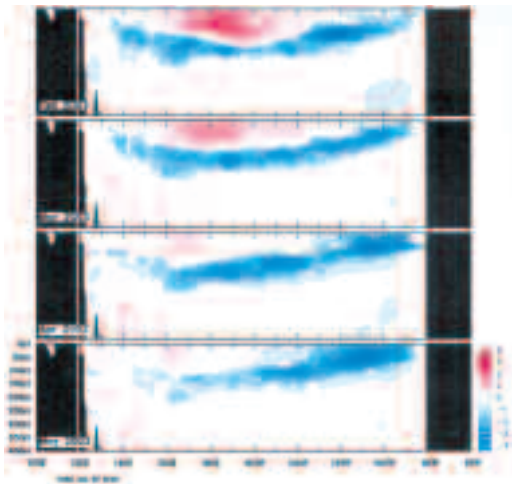
Fig. 4 Time-longitude section of the monthly anomalous depth of the  $20^{\circ}\text{C}$  isotherm at the equator from January 1996 to May 2003. The contour interval is 10 m.



Reid (2003) noted that sub-surface data at the end of summer suggested that the El Niño which formed in autumn 2002, was close to ending. In autumn 2003, the evidence from the Pacific sub-surface unequivocally showed the event coming to an end. The depth of the thermocline became shallower than average (i.e. closer to the surface) over most of the tropical Pacific by the end of autumn. This can be seen in Fig. 4 by the presence of negative anomalies in the depth of the  $20^{\circ}\text{C}$  isotherm from  $170^{\circ}\text{E}$  to the South American coast during May 2003. These negative anomalies reached a minimum of  $-20$  to  $-30$  m in the far eastern Pacific in May.

Figure 5 shows a sequence of equatorial Pacific vertical temperature anomaly profiles for the four months ending May 2003, also obtained from the BMRC. In the figure, red (blue) shades indicate sub-surface waters which are warmer (cooler) than average. These diagrams show the reduction of both the intensity and strength of the El Niño-related warm anomaly in the central Pacific. By May, only a tiny remnant of this excess warmth remained in the western Pacific near  $160^{\circ}\text{E}$ . In contrast to the collapse of the warmth, negative anomalies intensified near the thermocline in the central and eastern Pacific. The extent of this cooling was at its greatest during April as May saw a reduction in both the intensity and vertical extent of the negative anomalies between  $170^{\circ}\text{E}$  and  $160^{\circ}\text{W}$ .

**Fig. 5** Four-month February to May 2003 sequence of vertical temperature anomalies at the equator for the Pacific Ocean. The contour interval is 0.5°C.



The decay of the El Niño event during the southern autumn, giving it a life-span of about twelve months, was similar to that observed in most previous events (see for example, Wang 2002 or Chan and Xu 2000).

As mentioned earlier, the cooling of the subsurface led to some speculation as to the likelihood of a La Niña event in 2003. (Historically, around 45 per cent of decaying El Niño events have evolved directly into a La Niña). Comparing this sequence with the corresponding period in 1998 (a period of transition from El Niño to La Niña), shows that the development of negative subsurface anomalies following the 1997/98 El Niño was much stronger than that which occurred in 2003 (Courtney 1998). The cold subsurface water in 1998 eventually gave rise to the 1998/99 La Niña (Beard 1999).

## Atmospheric patterns

### Surface analyses

The autumn 2003 mean sea-level pressure (MSLP) across the southern hemisphere is shown in Fig. 6, with the associated anomalies shown in Fig. 7. These anomalies are the departures from an eleven-year (1979-1989) climatology obtained from the European Centre for Medium-range Weather Forecasts (ECMWF). The MSLP analysis itself has been computed using data obtained from the Bureau of Meteorology's Global Assimilation and Prediction (GASP) model daily 0000 UTC analyses.

**Fig. 6** Autumn 2003 mean sea-level pressure (hPa). The contours are spaced at 5 hPa intervals.

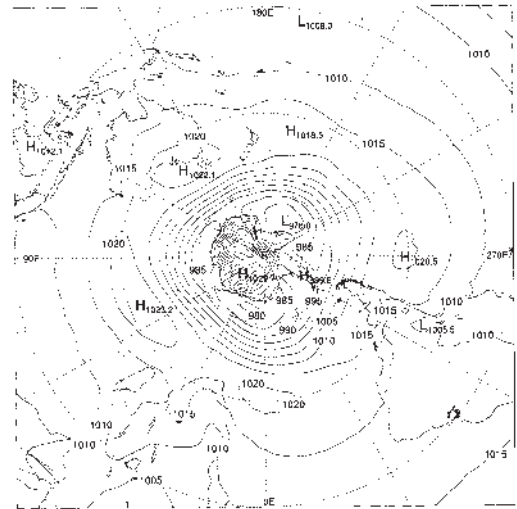
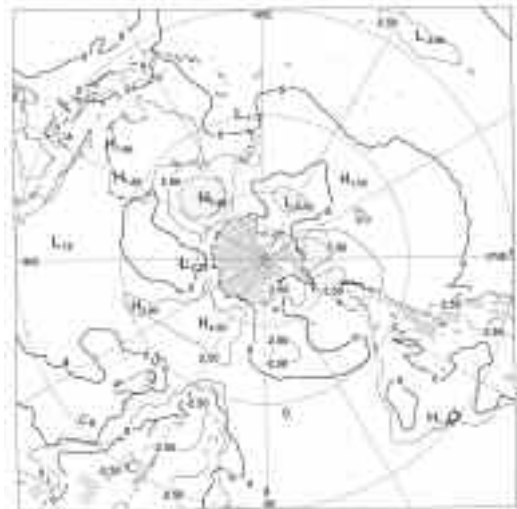


**Fig. 7** Autumn 2003 mean sea-level pressure anomaly (hPa). The contours are spaced at 2.5 hPa intervals.



The Antarctic circumpolar trough showed three substantial minima, located at 15°E, 100°E and 150°W. These centres of low pressure produced a three-wave pattern in the seasonal mean which showed great intraseasonal stability; that is, there was a high level of consistency from month to month. The very long wavelength between the Pacific trough and the Atlantic trough was compensated somewhat by the strong westward lean in the latter towards more

northern latitudes. Inspection of the individual monthly means shows that the March pattern was the most different from the seasonal mean, particularly near the Antarctic coast where MSLP was above average across all longitudes, with the exception of a small sector from 40°E to 60°E.

Most of Australia came under the influence of an anomalous ridge aligned north-south through the centre of the continent, and extending southward to the Antarctic coast. The peak anomaly within this feature was about +8 hPa near 50°S. The ridge represented a significant impediment to the mid-latitude westerlies which typically become an increasingly important source of rainfall for southern Australia as autumn progresses.

MSLP was below average over nearly all the tropical and subtropical Pacific with anomalies dropping to below -2 hPa just north of the equator between 150°W and 130°W. This situation was consistent with the persistence of negative SOI values discussed earlier. Another weak low pressure anomaly (-1 hPa) was situated just north of New Zealand.

### Mid-tropospheric analyses

The mean 500 hPa geopotential height patterns for autumn 2003 are shown in Fig. 8, with anomalies shown in Fig. 9. The three-wave characteristics in the MSLP pattern (Fig. 6) were also present in the mid-latitude flow (Fig. 8), with the troughs located in similar positions. The mean field showed a split in the flow across southern and southeastern Australia with a weak trough located over the Tasman Sea. A cyclonic anomaly (centre -26 m) was located in the same area with negative anomalies extending over parts of eastern Australia. Elsewhere over the country, 500 hPa height anomalies were weakly positive.

As with the surface pressure anomalies, the strongest feature in the hemisphere was the anticyclonic centre (+85 m) well south of Australia. This was located almost directly above the corresponding surface anomaly indicating a barotropic atmosphere.

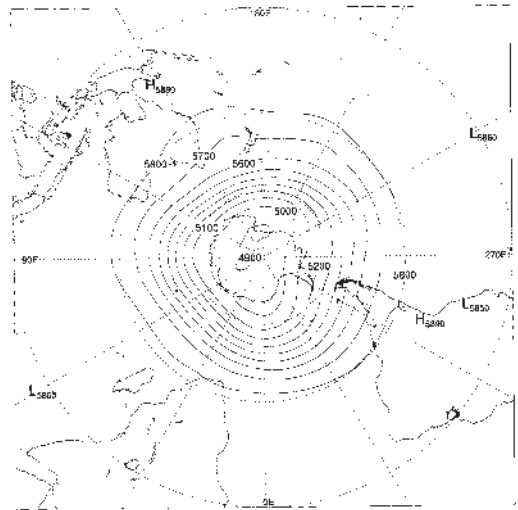
### Blocking

Figure 10 is a time-longitude section of the daily southern hemisphere mid-level Blocking Index:

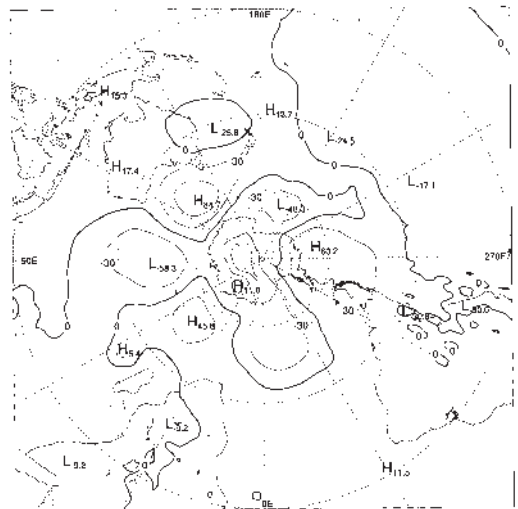
$$BI = 1/2[(u_{25} + u_{30}) - (u_{40} + 2u_{45} + u_{50}) + (u_{55} + u_{60})].$$

Here,  $u_{\lambda}$  indicates the 500 hPa level zonal wind component at  $\lambda$  degrees of southern hemisphere latitude ranging from 0° at the equator to +90°S at the South Pole. The blocking index measures the strength of the 500 hPa flow at the mid-latitudes (40°S to 50°S) relative to that at subtropical (25°S to 30°S) and high (55°S to 60°S) latitudes.

**Fig. 8** Autumn 2003 500 hPa mean geopotential height (m). The contours are spaced at 100 geopotential metre intervals.



**Fig. 9** Autumn 2003 500 hPa mean geopotential height anomaly (m). The contours are spaced at 30 geopotential metre intervals.



Taken across the entire season in the form of a seasonal mean (Fig. 11), blocking was above average from about 40°E through Australian longitudes to about 220°E (140°W). This is consistent with the positive 500 hPa height anomaly south of Australia as well as the split flow and upper low further to the east and northeast.

**Fig. 10** Autumn 2003 daily blocking index ( $\text{m s}^{-1}$ ): time-longitude section. The horizontal axis measures degrees of longitude east of the Greenwich meridian. Day one is 1 March.

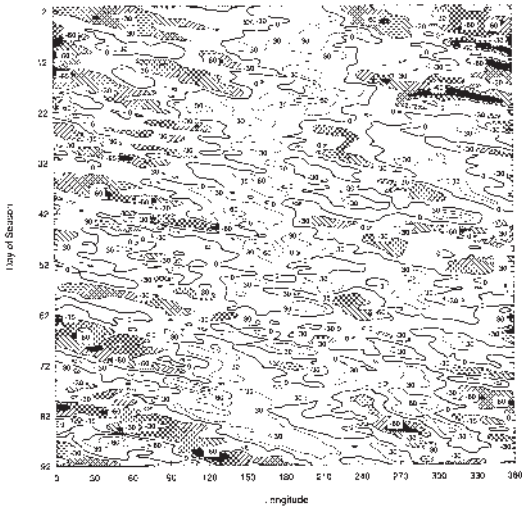
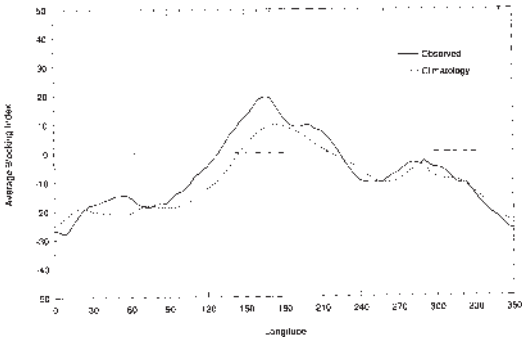


**Fig. 11** Mean southern hemisphere blocking index ( $\text{m s}^{-1}$ ) for autumn 2003 (solid line). The dashed line shows the corresponding long-term average. The horizontal axis shows degrees east of the Greenwich meridian.



The highest value of the BI for autumn was slightly over  $+90 \text{ m s}^{-1}$  near  $120^\circ\text{E}$  around the middle of May (day 77). The period when blocking was most persistent occurred during the first half of the season within about  $30^\circ$  of longitude of the date-line. In contrast, BI values generally remained low in the Atlantic and Indian Ocean sectors indicating highly mobile zonal flow, as is the climatological norm for this part of the hemisphere.

**Winds**

Low-level (850 hPa) and upper-level (200 hPa) wind anomalies for autumn 2003 are shown in Figs 12 and 13 respectively. Isotach contours are at  $5 \text{ m s}^{-1}$  intervals, and in Fig. 12 the regions of the globe where the land rises above 850 hPa are shaded grey. The low-level pattern in the central Pacific shows a slightly enhanced trade wind regime on both sides of the equator, while in the eastern equatorial Pacific the wind anomalies had similar magnitudes but were more meridional in nature. West of the date-line, the tropical Pacific 850 hPa anomalies were generally very small.

Low-level wind anomalies across Australia were mostly weak during autumn, the main exception being a band of easterly anomalies affecting the far southeast. These anomalies formed the northern flank of an anticyclonic anomaly centred over the Southern Ocean well south of eastern Australia, a feature consistent with the MSLP and 500 hPa anomalies discussed earlier. A cyclonic anomaly was observed over the north Tasman Sea, and there was another cyclonic circulation anomaly located southwest of WA, resulting in northwest to northeasterly anomalies across the west of that State.

The upper levels of the tropical Pacific were characterised by northwest to westerly anomalies south of the equator and east of about  $170^\circ\text{W}$ . Combined with the slightly stronger Trade Winds, the increased westerlies aloft indicated an enhanced Walker circulation; a sign that the 2002/03 El Niño had decayed. The individual monthly analyses (not shown) indicate that this pattern gradually became stronger and more coherent as the season progressed.

A series of anomalous upper level troughs and ridges affected the Australian region during autumn. Centres of cyclonic rotation were situated over the southern Indian Ocean and the west Tasman Sea, the latter being associated with an elongated trough extending north to northwest over Queensland and east-southeast towards New Zealand. An anomalous ridge was situated between the cyclonic centres with anticyclonic circulations being observed over northwest WA and well south of Australia. This latter feature coincided with similar MSLP and 500 hPa anomalies and was associated with a strong southward displacement of the polar front jet over Australian longitudes.

**Australian region**

**Rainfall**

Figure 14 shows the autumn rainfall totals for Australia, while Fig. 15 shows the autumn rainfall deciles, where the deciles are calculated with respect to gridded rainfall data for all autumns from 1900 to 2003.



**Fig. 14 Autumn 2003 rainfall totals (mm) in Australia.**

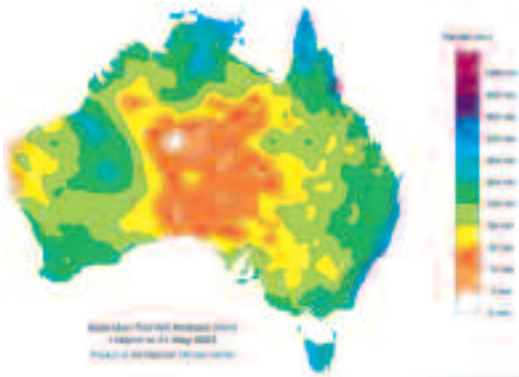
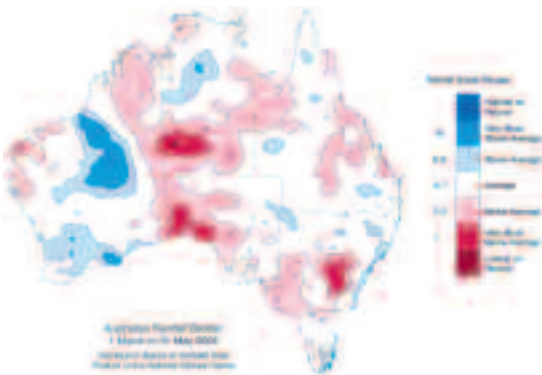


**Fig. 15 Autumn 2003 rainfall in Australia: decile range values based on grid-point values over the autumns 1900 to 2003.**



appointing, especially considering the widespread above average falls that occurred in February. Although March to May totals were generally close to the median over much of the drought-affected eastern half of the country, they were not sufficient to provide a genuine break, only some welcome relief.

In relative terms April was the wettest month of the season with only small areas registering falls below the 30th percentile. Large areas of northern NSW, southern and western Queensland and the adjacent far north of SA and far southeast of the NT recorded April rainfall totals above the 70th percentile. This was also the case for large parts of WA. March and May on the other hand saw large tracts of agriculturally important country recording below to very much below average rainfall.

Table 1 summarises the seasonal rainfall ranks and extremes on a national and State basis.

**Temperatures**

Figures 16 and 17 show the maximum and minimum temperature anomalies respectively for autumn 2003. The anomalies have been calculated with respect to the 1961-1990 period.

Maximum temperatures were above average for the season across large parts of the country (Fig. 16), apart from some of the heavily populated areas of the east and south. Large parts of western Queensland, the NT and southwest WA recorded anomalies between +1 and +2°C, the latter region having a few small patches in the +2 to +3°C range. Negative anomalies were weaker in magnitude, being generally in the range from 0 to -1°C. Much of South Australia recorded cooler than average maxima, as did a large area stretching from southeast Queensland across the eastern half of NSW to Gippsland in Victoria.

**Table 1. Autumn seasonal rainfall extremes and ranks on a national and State basis.**

	<i>Highest seasonal total (mm)</i>	<i>Lowest seasonal total (mm)</i>	<i>Highest 24-hour fall (mm)</i>	<i>Area-averaged rainfall (AAR) (mm)</i>	<i>Rank of AAR *</i>
Australia	1809 at Bellenden Ker Top Station (QLD)	Zero at several locations (NT)	261.0 at Tree House Creek on 14 March (QLD)	93	30
WA	344 at Dwellingup	3 at Exmouth Town	175.0 at Telfer on 1 March	91	58
NT	469 at Bickerton Island	Zero at several locations	164.0 at Ramingining on 12 March	92	36
SA	266 at Myponga	2 at Marree	95.8 at Myponga on 24 May	27	20
QLD	1809 at Bellenden Ker Top Station	5 at Roseberth Station	261.0 at Tree House Creek on 14 March	113	36
NSW	1062 at Ballina	8 at Turlee	183.0 at Forster Beach on 15 May	116	58
VIC	409 at Wylangta	14 at Lake Boga	83.2 at Casterton on 20 March	110	29
TAS	753 at Mount Read	79 at Yambacoona	149.0 at Golden Valley on 13 April	287	74

\* The rank goes from 1 (lowest) to 114 (highest) and is calculated on the years 1890 to 2003 inclusive.

**Fig. 16 Autumn 2003 maximum temperature anomalies (°C) for Australia based on a 1961-1990 mean.**

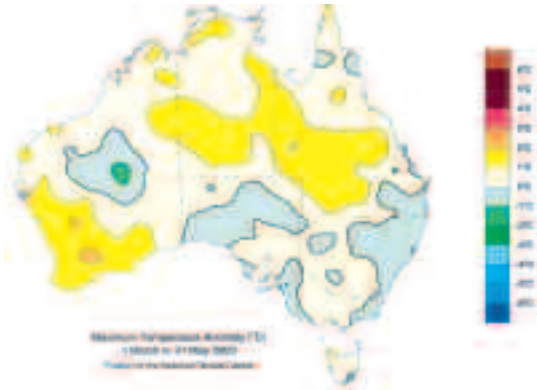
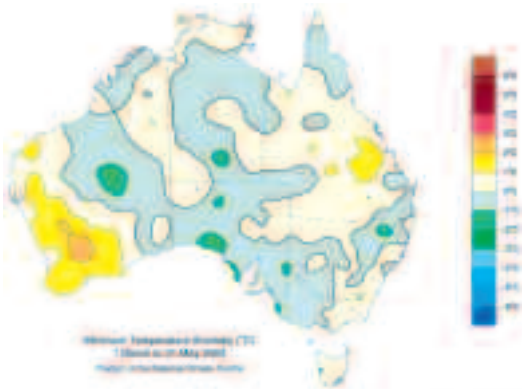


**Fig. 17 Autumn 2003 minimum temperature anomalies (°C) for Australia based on a 1961-1990 mean.**



Positive maximum temperature anomalies became progressively more widespread as the season progressed, so that by May the only region with below average maxima was a small patch in far western NSW. The national area-averaged maximum temperature anomalies were  $-0.22$ ,  $+0.88$  and  $+1.26$  for March, April and May respectively. May's value was the sixth-highest in the post-1950 period.

Autumn minimum temperatures (Fig. 17) were closely balanced between positive and negative anomalies. In similar fashion to the maximum temperatures, the strongest positive anomalies in the seasonal minima occurred in southwest WA where the

range was  $+1$  to  $+3^{\circ}\text{C}$ . Minimum temperatures were also mainly above average in Queensland where there were a few areas with  $+1$  to  $+2^{\circ}\text{C}$  anomalies, and across all of Tasmania. In contrast weak negative anomalies ( $0$  to  $-1^{\circ}\text{C}$ ) dominated in the NT, eastern WA, most of SA, western Victoria and both southwest and northeast NSW. There were several small patches with departures in the  $-1$  to  $-2^{\circ}\text{C}$  range.

In terms of the monthly patterns, March stood out again as the most anomalously cool with large areas of the nation recording negative anomalies, including significant areas in the  $-1$  to  $-2^{\circ}\text{C}$  range. The national area-averaged minimum temperature anomalies were  $-0.73$ ,  $+0.57$  and  $+0.58$  for March, April and May respectively.

Table 2 summarises the seasonal maximum temperature ranks and extremes for autumn on a national and state basis, and Table 3 shows a corresponding analysis for the seasonal minimum temperatures.

## References

- Beard, G. 1999. Seasonal climate summary southern hemisphere (spring 1998): a weak, but intensifying, cold event (La Niña) in the Pacific basin. *Aust. Met. Mag.*, 48, 133-40.
- Bureau of Meteorology 2003. *Climate Monitoring Bulletin - Australia*, March, April and May 2003 issues. National Climate Centre, Bur. Met., Australia.
- Bureau of Meteorology 2003. *Monthly Rainfall Review - Australia*, April 2003 issue. National Climate Centre, Bur. Met., Australia.
- Bureau of Meteorology 2003. *South Pacific Seasonal Outlook Reference Material*, Number 36 - April 2003 issue. National Climate Centre, Bur. Met., Australia.
- Chan, J.C.L. and Xu, J. 2000. Physical Mechanisms Responsible for the Transition from a Warm to a Cold State of the El Niño-Southern Oscillation. *Jnl Climate*, 13, 2056-71.
- Climate Prediction Centre 2003. *Climate Diagnostics Bulletin*, March, April, May 2003 issues. US Department of Commerce, National Oceanic and Atmospheric Administration, Washington D.C.
- Courtney, J. 1998. Seasonal climate summary southern hemisphere (autumn 1998): decline of a warm episode (El Niño). *Aust. Met. Mag.*, 47, 339-46.
- Fawcett, R.J.B. and Trewin, B.C. 2003. Seasonal climate summary southern hemisphere (autumn 2002): onset of El Niño conditions. *Aust. Met. Mag.*, 52, 127-36.
- Reid, P.A. 2003. Seasonal climate summary southern hemisphere (summer 2002/03): El Niño begins its decline. *Aust. Met. Mag.*, 52, 265-76.
- Wang, C. 2002. Atmospheric circulation cells associated with the El Niño-Southern Oscillation. *Jnl Climate*, 15, 399-419.
- Wheeler, M. and Weickmann, K.M. 2001. Real-time monitoring and prediction of modes of coherent synoptic to intraseasonal tropical variability. *Mon. Weath. Rev.*, 129, 2677-94.
- Wolter, K. and Timlin, M.S. 1993. Monitoring ENSO in COADS with a seasonally adjusted principal component index. *Proc. of the 17th Climate Diagnostics Workshop*, Norman, OK, NOAA/NMC/CAC, NSSL, Oklahoma Clim. Survey, CIMMS and the School of Meteor., Univ. of Oklahoma, 52-7.
- Wolter, K. and Timlin, M.S. 1998. Measuring the strength of ENSO - how does 1997/98 rank? *Weather*, 53, 315-24.

**Table 2. Autumn seasonal maximum temperature extremes and ranks on a national and State basis.**

	<i>Highest seasonal mean (°C)</i>	<i>Lowest seasonal mean (°C)</i>	<i>Highest daily recording (°C)</i>	<i>Lowest daily recording (°C)</i>	<i>Anomaly of area-averaged mean (°C) (AAM)</i>	<i>Rank of AAM *</i>
Australia	36.3 at Fitzroy Crossing (WA)	8.4 at Mount Wellington (TAS)	45.5 at Roebourne on 18 March (WA)	0.0 at Crackenback on 1 March (NSW) and at Mt Hotham on 16 April (VIC)	+0.64	46
WA	36.3 at Fitzroy Crossing	10.4 at Bridgetown	45.5 at Roebourne on 18 March	12.2 at Newdegate on 31 May	+0.71	40
NT	35.6 at Bradshaw	28.0 at Kulgera	41.0 at Wulungurru on 18 March	7.7 at Kulgera on 14 May	+0.88	46
SA	28.9 at Marree	15.8 at Mount Lofty	39.7 at Marla on 18 March	8.6 at Mount Lofty on 27 May	+0.20	28
QLD	34.1 at Camooweal	20.4 at Stanthorpe	42.4 at Bedourie on 18 March	5.0 at Stanthorpe on 22, 27 and 29 May	+0.93	48
NSW	28.0 at Mungindi	10.0 at Crackenback	39.0 at Tibooburra Airport on 18 March	0.0 at Crackenback on 1 March	+0.12	33
VIC	23.9 at Mildura	9.1 at Mt Hotham	35.7 at Mildura and Geelong on 18 March	0.0 at Mt Hotham on 16 April	+0.29	39
TAS	19.3 at Bridport	8.4 at Mount Wellington	32.0 at Orford on 18 March	0.6 at Mt Wellington on 3 May	+0.06	32

\* The temperature ranks go from 1 (lowest) to 54 (highest) and are calculated on the years 1950 to 2003 inclusive.

**Table 3. Autumn seasonal minimum temperature extremes and ranks on a national and State basis.**

	<i>Highest seasonal mean (°C)</i>	<i>Lowest seasonal mean (°C)</i>	<i>Highest daily recording (°C)</i>	<i>Lowest daily recording (°C)</i>	<i>Anomaly of area-averaged mean (°C) (AAM)</i>	<i>Rank of AAM *</i>
Australia	26.7 at Troughton Island (WA)	0.6 at Crackenback (NSW)	29.4 at Paraburdoo on 20 March (WA)	-7.3 at Glen Innes on 23 May (NSW)	+0.14	38
WA	26.7 at Troughton Island	10.4 at Bridgetown	29.4 at Paraburdoo on 20 March	0.0 at Yeelirrie on 29 May	+0.54	41
NT	26.0 at McCluer Island	11.5 at Alice Springs	29.0 at Warruwi on 4 March	1.3 at Alice Springs on 29 May	-0.15	27
SA	15.3 at Moomba	7.4 at Yongala	24.0 at Moomba on 7 March	-3.0 at Naracoorte Airport on 5th May	-0.22	27
QLD	25.8 at Coconut Island	9.4 at Stanthorpe	29.0 at Coconut Island on 1 March	-3.0 at Stanthorpe on 23 May	+0.11	34
NSW	16.3 at Yamba	0.6 at Crackenback	25.8 at White Cliffs on 19 March	-7.3 at Glen Innes on 23 May	+0.02	29
VIC	13.8 at Gabo Island	2.8 at Mt Hotham	24.6 at Melbourne on 19 March	-4.7 at Mt Hotham on 4 May	-0.37	27
TAS	12.7 at Swan Island	2.0 at Liawenee	19.8 at Flinders Island on 19 March	-7.2 at Liawenee on 11 May	+0.45	48

## Appendix

Data sources used for this review were:

- National Climate Centre, *Climate Monitoring Bulletin - Australia*. Obtainable from the National Climate Centre, Commonwealth Bureau of Meteorology, GPO Box 1289K, Melbourne, Vic. 3001, Australia.
- National Climate Centre, *Monthly Rainfall Review - Australia*. Obtainable from the Publications Section, Commonwealth Bureau of Meteorology, GPO Box 1289K, Melbourne, Vic. 3001, Australia.
- Climate Prediction Center (CPC), *Climate Diagnostics Bulletin*. Obtainable from the Climate Prediction Center (CPC), National Weather Service, Washington D.C., 20233, USA.

